

6-W Optical Power Link With Integrated Optical Data Transmission

Henning Helmers , Cornelius Armbruster, Moritz von Ravenstein , David Derix, and Christian Schöner

Abstract—This article demonstrates a fiber-based power-by-light system that is capable of delivering up to 6.2 W of continuous electrical power at common voltages of 3.3 and 5 V. This optical link includes bidirectional optical communication, for which the data stream from the base to the remote unit is realized by amplitude modulation of the laser beam over the same fiber. At the remote unit, a gallium arsenide-based photovoltaic (PV) laser power converter receives and converts the light. The data are demodulated with a dedicated electric circuit, while the power is forwarded to a dc–dc boost converter. The optical data uplink is realized over a separate optical fiber. In operation, a PV conversion efficiency of above 50% has been measured. For downlink data rates up to 115.2 kb/s, unperturbed signal integrities are demonstrated, at higher data rates, the signal integrity deteriorates. An assessment of power budget and power losses in the overall system is presented. Finally, a smart power management concept is introduced, which controls the laser output power with respect to changing electrical load, optimizes the operating point of the PV cell, and, thus, increases system efficiency for varying load operation. Thereby, it also minimizes laser and PV cell operating temperatures, and eventually prolongs the lifetime of the system.

Index Terms—Photovoltaic cells, lasers, power transmission, optical communication, amplitude modulation, optical receivers, laser applications, optical fibers, dc-dc power converters, energy management, power transmission.

I. INTRODUCTION

OPTICAL power transmission is an elegant way to supply power to sensors, actuators, and other electrical consumers with high isolation demands. Compared with conventional copper wiring, this technology provides unique benefits, such as galvanic isolation, avoidance of electromagnetic interference, replacement of copper cables with low-weight fiber, avoidance of electric sparks while ensuring highest reliability and the possibility for wireless power transmission through free space. Thereby, it enables new applications in various domains (e.g., power supply for gate-drivers, probes, or sensors in high-voltage environment [2]–[7], ripple-free opto-couplers

Manuscript received September 12, 2019; revised December 13, 2019; accepted January 12, 2020. Date of publication January 16, 2020; date of current version April 22, 2020. This work was presented in part at the 1st Optical Wireless and Fiber Power Transmission Conference (OWPT2019), Yokohama, Japan, April 2019 [1]. Recommended for publication by Associate Editor L. Chang. (Corresponding author: Henning Helmers.)

The authors are with the Fraunhofer Institute for Solar Energy Systems ISE, Freiburg 79110, Germany (e-mail: henning.helmerts@ise.fraunhofer.de; cornelius.armbruster@ise.fraunhofer.de; moritz.von.ravenstein@ise.fraunhofer.de; david.derix@ise.fraunhofer.de; christian.schoener@ise.fraunhofer.de).

Color versions of one or more of the figures in this article are available online at <https://ieeexplore.ieee.org>.

Digital Object Identifier 10.1109/TPEL.2020.2967475

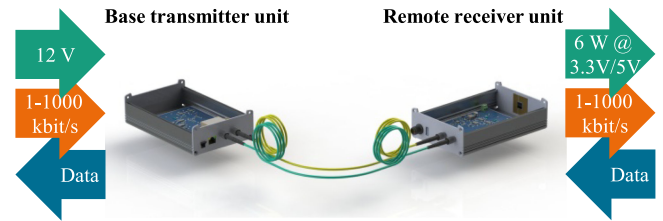


Fig. 1. Visualization of the system.

[8], optically powered networks [9], [10], optical powering of remote antenna units [11], [12], magnetic-resonance compatible active implants [13], wireless powering of medical devices from outside the body [14]–[16], lightning-safe power supply for wind turbine structural health monitoring systems [17], and wireless powering of consumer electronics [18]). An interesting extension of power-by-light technology, or power-over-fiber when optical fiber is used as a waveguide, is the combination with optical communication (also known as simultaneous wireless information and power transfer). To facilitate market penetration, the integration of power and data transmission into a single fiber and a reduction in number of required costly optoelectronic components and related optical coupling are of great interest [19].

This article demonstrates the development and evaluation of an optical power transmission system with integrated bidirectional optical data transmission. As a first step toward integration of power and data, here, the data downlink from base transmitter unit to remote receiver unit is realized by amplitude modulation, i.e., the photovoltaic (PV) cell is used as a receiver for power and data at the same time. The system configuration of this system is reported in detail in Section II. In Section III, experimental measurement results and a power loss analysis is discussed. Finally, in Section IV, a smart power management scheme is introduced, which allows for minimizing the laser output power based on the power demand of the load at the remote unit.

II. SYSTEM CONFIGURATION

The developed optical link consists of a base transmitter unit and a remote receiver unit connected by two optical fibers, as shown in Fig. 1. Both units feature generic external interfaces. An overview of the system specifications is given in Table I.

A. Base Transmitter Unit

The block diagram of the functional building blocks including power and data stream on the base unit is shown in Fig. 2. The

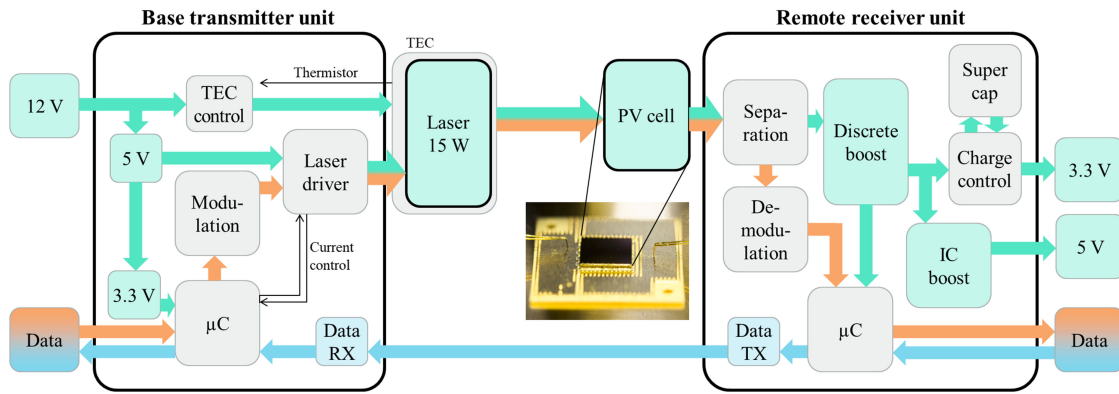


Fig. 2. Block diagram of the system consisting of base transmitter unit and remote receiver unit.

TABLE I
SYSTEM SPECIFICATIONS

Input voltage	12 V
Output power	up to 6.2 W
Output voltage	3.3 V and 5 V
Data downlink (base to remote)	up to 1000 kbit/s modulated onto power downlink
Data uplink (remote to base)	separate fiber for data uplink
Laser	Fiber-coupled diode laser (809 nm, up to 15 W power output at fiber end)
Fiber	Multimode, length: 1.5 m, numerical aperture: 0.22, core diameter: 400 μm
PV cell	GaAs based PV laser power converter, 10x10 mm ²

base unit is driven by a 12-V external power supply. The 12 V are down-converted on-board into 5 and 3.3 V using commercially available integrated circuit (IC) converters. Bidirectional data are received and transmitted in a digital form.

The base unit hosts the laser driver and is connected to a fiber-coupled diode laser (809 nm, optical power output up to 15 W at fiber end). The laser driver is capable of analog and digital modulation of the laser diode output up to 200 MHz. In this article, analog modulation up to 1000 kHz controlled by the microcontroller (μC) has been applied. A thermoelectric cooler (TEC) with integrated thermistor and a separate control circuit are used to maintain a constant laser diode temperature in operation of 25 °C. A separate photodiode (data RX in Fig. 2) receives incoming data from the remote unit, which is forwarded through the μC to the external digital data interface.

B. Signal Amplitude Modulation

The μC uses the Infrared Data Association (IrDA) protocol to transmit the digital data input. The IrDA protocol is chosen due to its low power consumption and broad range of supported data rates (kb/s to Gb/s). The conventional IrDa signal is shown in Fig. 3(a). To increase the average output power, the IrDA signal is modified for the amplitude modulation as follows [see Fig. 3(b)]: 1) the signal is flipped, 2) the pulsewidth T_{pulse} is shortened from 3/16 of the bit length T_{bit} to 100 ns, and 3) the modulation depth is reduced from 1 to 2/3, i.e., the laser does

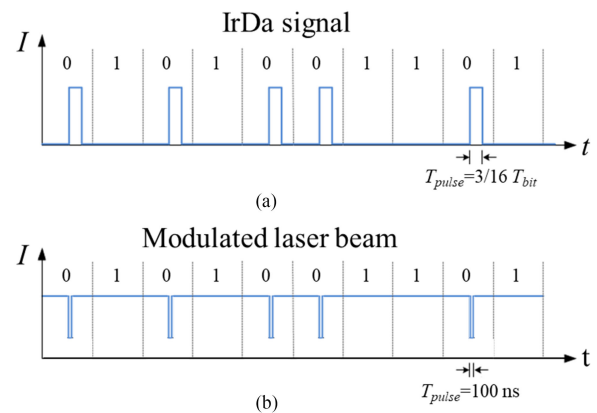


Fig. 3. Illustration of the IrDA signal modification. Plotted is the amplitude I over time t .

not shut off completely with “0” bit, but instead only drops to one-third of the power. It should be noted that the signal-to-noise ratio at the receiver is expected to be influenced by both bit length and modulation depth, and is data rate dependent. However, a thorough optimization in that regard was outside the scope of this article.

C. Remote Receiver Unit

The remote unit hosts the PV cell for power conversion and data reception as well as downstream electronics for data processing, power management, voltage conversion, and data transmission. In order to enable generic application, the remote unit provides constant power supply at two external terminals at common voltage levels of 3.3 and 5 V. The block diagram of the remote receiver unit and its functional elements is shown in Fig. 2.

A 10 × 10 mm² gallium arsenide (GaAs)-based PV cell, which has been developed and fabricated at Fraunhofer ISE, is used for laser power conversion. The front grid structure features parallel grid lines (comb design) designed for operation under high intensity to extract currents up to 10 A. The nominal designated area is $A_{\text{des}} = 0.978 \text{ cm}^2$. The PV cell is mounted on a 29 × 29 mm² metalized ceramic submount guaranteeing electrical isolation while providing good thermal contact to

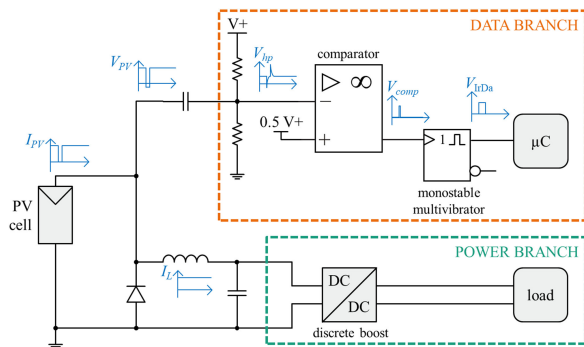


Fig. 4. Schematic representation of the separation circuit at the remote receiver which divides the PV cell output into an ac data branch and a dc power branch.

the aluminum housing for effective passive heat dissipation. The backside contact of the PV cell is established by vacuum soldering of the chip onto a contact pad on the submount, the front side of the cell is contacted by thin Au wire bonding on two opposite sides of the PV. A picture of the mounted PV cell contacted on a measurement chuck is shown in Fig. 2. It should be noted that the PV cell has not been designed to operate as a data receiver, but has been selected to be able to receive and convert the optical power of up to 15 W. Especially, since the junction capacitance scales with area, a smaller PV cell is advantageous from data reception point of view [20]. However, then increasing current density and associated resistive losses as well as proper optical coupling to a smaller receiver would need to be carefully taken into consideration.

The PV cell output couples into a separation circuit, which separates the modulated data signal from the constant power response. A schematic representation of the circuit and the respective current and voltage signals are illustrated in Fig. 4. An inductor is used to achieve sufficiently high impedance so that alternating signals cannot propagate into the power path. When a “0” bit interrupts the otherwise constant PV current I_{PV} , the inductor maintains the current flow to the power path for this short period. At the same time, a negative voltage spike V_{PV} occurs at the PV cell, which carries the bit information. The data path is ac coupled using a high-pass filter. Behind the filter, the negative edge of the voltage spike is detected by a comparator and translated into a clear pulse signal. This pulse is, then, stretched by a monostable multivibrator to meet the specification of the IrDA to enable processing by the μC . Finally, the μC forwards the data to the digital external interface. For the uplink of remote data back to the base, the digital external data are forwarded by the μC to a conventional vertical-cavity surface-emitting laser transmitter, shown as data TX in Fig. 2.

The power branch behind the separation circuit consists of a boost converter, which provides 3.3 V, as shown in “discrete boost” in Figs. 2 and 4, a supercapacitor for energy storage (100 Ws to maintain at least 20 s of operation in case of a link breakdown) and related charge controller, and a second boost converter to provide the additional 5 V output, as shown in “IC boost” in Fig. 2. For the first stage conversion from the PV output voltage to 3.3 V, a compact boost converter based on gallium nitride (GaN) transistors has been developed

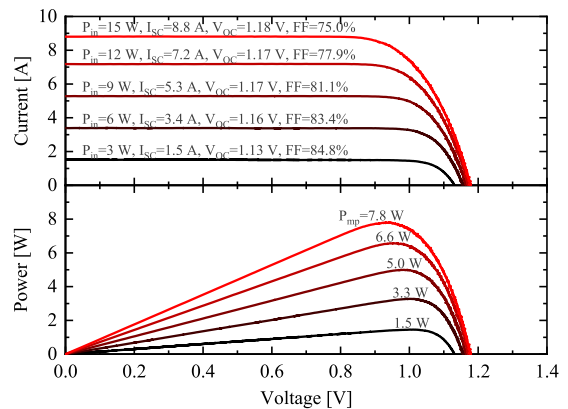


Fig. 5. Current-voltage (top) and power-voltage (bottom) characteristics of the GaAs-based PV cell under continuous illumination with 809 nm laser light at different optical power levels P_{in} between 3 and 15 W. The short-circuit current I_{SC} , open-circuit voltage V_{OC} , maximum power P_{mp} , and fill factor FF are stated with each curve.

and realized with discrete components. It is based on an interleaved boost topology with a switching frequency of 250 kHz, details on the design and layout of GaN based dc-dc converters have been published elsewhere [21], [22]. For input currents up to 8 A, it boosts from start-up voltages between $V_{in} = 0.85$ V and $V_{in} = 1$ V to a constant output voltage of $V_{out} = 3.3$ V. As the name suggests, for the second stage boost from 3.3 to 5 V a commercial IC [23] has been used.

III. PERFORMANCE MEASUREMENTS

To investigate the performance of the system, the subunits have been characterized both individually and as a complete system. The laser power at the end of the 1.5-m long optical fiber has been measured with an optical power meter for various driving currents. The PV cell’s current- and power-voltage characteristics, as plotted in Fig. 5, have been measured separately at different optical input power under illumination with the 809 nm laser light coupled from the fiber to the PV cell (approximately Gaussian profile). The output power of the PV cell in operation, which corresponds to the input power of the electronics of the remote unit, has been measured using an oscilloscope and a clamp-on ammeter. Thereby, additional impedances between PV cell and electronics caused by the measurement itself have been avoided. The dc-dc boost converter as a subunit has been characterized with a precision power analyzer for different input voltages. The electrical input power at the base unit’s external interface and the electrical output power at the remote unit’s external interface have been measured with a precision power analyzer, results are presented in the following sections.

A. Discrete DC-DC Boost Converter

The measured conversion efficiency of the discrete dc-dc boost converter as single stage (i.e., without the additional downstream “IC boost” converter) at the remote unit is shown in Fig. 6. At $V_{in} = 1$ V and an electrical power output of 2.45 W, a peak efficiency of 86.2% is reached. At lower power, the efficiency drops due to relatively higher auxiliary power demand mainly

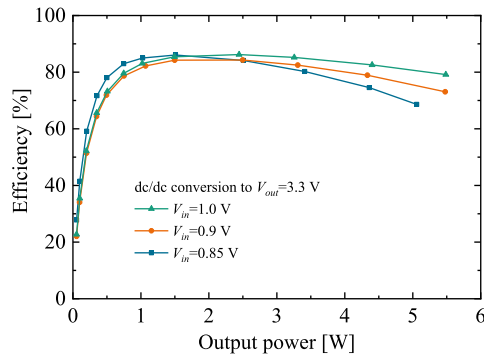


Fig. 6. Measured efficiency curves of the discrete boost converter for different input voltage levels V_{in} and a constant output voltage $V_{out} = 3.3$ V.

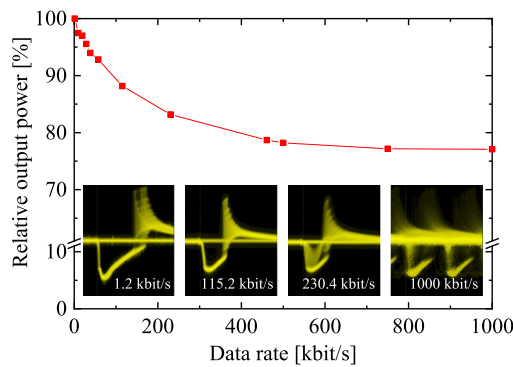


Fig. 7. Measured delivered output power at 3.3 V constant output voltage as a function of data rate for a modulation depth of $2/3$. The relative power at 100% here amounts to 6.2 W (the measured power at 1 kb/s). The insets show the eye diagrams of V_{hp} at different data rates. All eye diagrams represent a time interval of $2.4 \mu\text{s}$.

for gate drive circuit supply, at higher power, the efficiency drops due to increasing Joule heating. For lower input voltages, the drop at high power operation is more pronounced because of the related higher currents at the same power levels. For $V_{in} = 0.85$ V, the efficiency peak is shifted toward lower power, which is a result of the reduction of gate driving losses at these low voltage and low power operating conditions.

B. Power and Data Performance

At transmission of random data at a low data rate of 1.2 kb/s, a constant electrical power output of 6.2 W at 3.3 V stable voltage output is measured. Beyond this, data transmission with data rates up to 1000 kb/s has been tested. With increasing data rate, a drop in the delivered output power at the external terminal is observed. The measured dependence of the output power on the transmitted data rate is shown in Fig. 7. The observed drop may be attributed to the increasing power budget required for demodulation and processing of the data stream. The insets in Fig. 7 show eye diagrams of V_{hp} , i.e., the voltage signal that enters the ac branch behind the high-pass filter (see Fig. 4), for four example data rates. At low data rate of 1.2 kb/s, the eye is clearly open, each “0” bit is well detected by the distinguished negative flank at the beginning of the pulse. The same still holds true for an elevated data rate of 115.2 kb/s. At 230.4 kb/s, the eye begins to close, i.e., not all “0” bits lead to the same

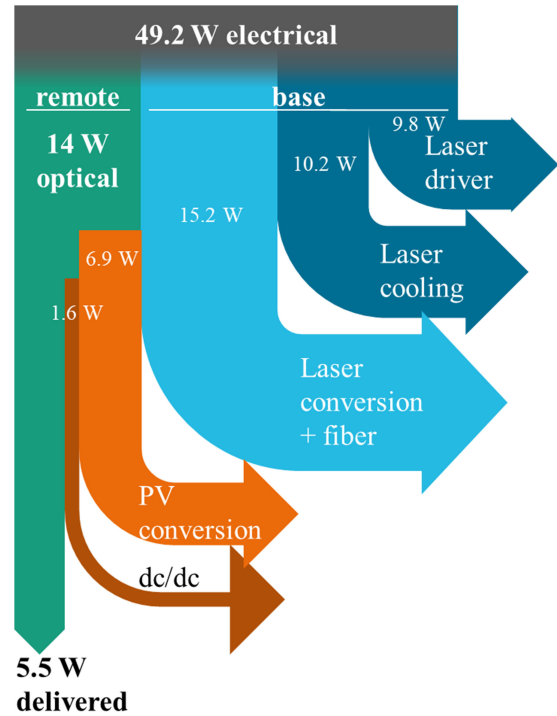


Fig. 8. Sankey diagram of the optical power link, starting with electrical power input, power budget on base transmitter unit, optoelectrical conversion, power budget on remote receiver unit, to final delivered electrical output power. The shown data represents the case of 5.5 W delivered power at output voltage of 3.3 V with simultaneous data transmission over the same optical link at a data rate of 1 kb/s.

voltage pulse, which indicates that signal integrity deteriorates. At 1000 kb/s, the overshoot of one pulse clearly extends into the next pulse. Hence, proper pulse detection poses a challenge. Still, advanced flank detection, signal processing schemes, and data transmission protocols may be sufficient to operate properly with these pulses.

C. Power Budget and Loss Analysis

To understand the power budget of the optical link as a whole and its subunits, a respective loss analysis for continuous operation at a delivered output power of 5.5 W and data rate of 1 kb/s has been performed. The results of this analysis for the case of 14 W optical laser power on the PV cell are visualized in form of a Sankey diagram, as shown in Fig. 8.

The electrical power consumption at the 12 V input of the base transmitter unit is 49.2 W. The largest fraction of this power is consumed at the transmitter side of the optical link, namely for the laser driver circuit including the amplitude modulation for integrated data transmission (9.8 W), thermoelectric cooling of the diode laser (10.2 W), and the laser electrical-to-optical power conversion and losses in the fiber (15.2 W). Consequently, the PV cell is irradiated with 14.0 W of optical power. The measured PV conversion efficiency in continuous operation varied between 51% and 54%. A comparatively small amount of the remaining fraction relates to optical losses at the PV cell, namely metal grid shading of the irradiated area (approximately 10%) and reflection of the laser light at the front surface of the active PV

cell area (<1%). The majority of the power loss is related to heat generated inside the PV cell. It is remarked that this heat generation is affecting the performance of the optical power link in two ways. First, as it relates back to nonunity efficiency of the optical-to-electrical conversion by the PV cell, it limits the delivered electrical output of the link. Second, in continuous operation, the heat must be effectively dissipated. The effective thermal resistance between PV cell and heat sink (i.e., in the usual case of passive cooling given by the environment) defines the temperature rise of the PV cell in operation. And with increasing operating temperature, the conversion efficiency drops and results in an even further increased heat generation.

IV. SMART POWER MANAGEMENT

In many applications, for optical power transmission, the load profile is not constant and, thus, the externally requested power for the presented system will often be below the maximum delivered power. Therefore, here we introduce a smart power management procedure as follows.

The system starts with full laser power, so that also the PV cell photocurrent (or more precisely the light-induced shift of its current-voltage characteristics) is maximal. If the requested load power is below the power provided by the PV cell, the charge controller on the remote unit charges the on-board storage. The proposed power management is based on a feedback control between the charge controller on the remote unit and the laser driver on the base unit only (and the respective μ Cs involved for data processing and communication), i.e., no external controller is required. As long as the charge controller measures sufficient voltage at the supercapacitor, the laser power is incrementally reduced. This continues until the power provided by the PV cell drops below the requested power at the external terminal. To maintain constant power output, the remaining power is provided by the storage. As soon as the charge controller detects the related voltage drop there, the laser driver receives the command to increase the power again. Hence, with a respective control algorithm, which should be adapted to suit typical load variations, this procedure maintains continuous operation without affecting the security of delivering power to the load when it is needed. Yet, at the same time, the laser power is reduced to the minimum with respect to the load demand only.

This smart power management has several advantages for the overall system performance: Since the laser is driven at minimal power, the heat that needs to be dissipated by the TEC is minimized. Consequently, the power budget for laser cooling drops. Also, the laser diode junction temperature is reduced, which is beneficial for its electrical-to-optical conversion efficiency. Similarly, as only a minimum of optical power is transmitted, the generated heat at the PV cell is minimized as well. This results in a lower PV cell operating temperature, which, in turn, increases the optical-to-electrical conversion efficiency and output voltage since both these properties feature a negative temperature coefficient [24]. Finally, besides improved efficiencies, due to lower operating temperatures, the presented smart power management scheme leads to prolonged lifetimes of the components, especially the laser.

V. CONCLUSION

A purely optical system for combined power and bidirectional data transmission has been presented. The system is capable of continuous delivery of up to 6.2 W of electrical power at a voltage output of 3.3 and 5 V.

The link is based on a 809-nm fiber-coupled laser diode that is directed onto a GaAs-based PV laser power converter, with an efficiency in operation of above 50%. The downlink data stream (i.e., from base transmitter unit to remote receiver unit) is realized by amplitude modulation of the laser beam over the same fiber using a modified IrDA protocol. At the remote receiver unit, the data are demodulated with a separation circuit. The power is passed to a discrete dc-dc converter that boosts the comparatively low PV cell voltage of about 1–3.3 V to supply the external load as well as a small on-board energy storage. Thereby, a peak efficiency of 86.2% was reached. In addition, a second off-the-shelf boost converter provides additional 5 V external voltage output.

A maximum delivered power of 6.2 W has been realized at a downlink data rate of 1.2 kb/s. Beyond higher data rates up to 1000 kb/s have been tested, whereas this comes at the cost of delivered output power and deteriorating signal integrity. Unperturbed signals and clear pulses were measured for data rates up to 115.2 kb/s; at 230.4 kb/s, the signal integrity starts to deteriorate. For the uplink data stream from remote receiver unit to the base transmitter unit, a conventional optical communication link is implemented over a separate fiber. Hence, this article can be understood as a first step toward a fully integrated optical power and data transmission system over only one optical fiber [19].

It should be remarked that a significant boost in electrical performance is expected when the PV cell is replaced with more advanced structures with front lateral conduction layer [25] and a back mirror for photon recycling [26], [27]. Still, the low-loss extraction of high currents from cm^2 -sized PV cells remains a challenge. Regarding voltage conversion, the use of PV cells with integrated series connection, such as multijunction [28]–[35] or multisegment [32], [34], [36]–[38] cells, is an interesting option because of their elevated output voltages. Yet, the respective downsides, namely increased sensitivity against temperature variation [31], [34] and misalignment [39]–[41] need to be considered in light of the actual application. In addition, series-connected receivers are beneficial for data transmission, as the reciprocal capacitance of a string of subcells is given by the sum of the reciprocals of the subcells' capacitances. Further performance improvements of the system can be expected from optimization of laser driving circuit and thermal management on both base and remote units.

In addition to the presented hardware and its capabilities, a smart power management concept has been introduced, which is based on a simple feedback control loop between the charge controller of the storage and the laser driver. With respect to a varying external load, the procedure controls the laser power to a minimum value that meets the demand. In other words, contrary to a solar energy conversion system, not a fluctuating resource is managed by proper control of the load (maximum power point tracking), but rather a fluctuating load is managed by proper control of the laser. Thereby, it maximizes the overall

system efficiency, keeps temperatures of laser, and PV cell low resulting in prolonged lifetimes (mean time to failure) of the components. The latter is of special significance since current system lifetimes are typically limited by that of the laser diode.

ACKNOWLEDGMENT

The authors gratefully acknowledge the contributions of O. Kalmbach and M. Haid to the dc–dc boost converter development, system integration, and electrical performance measurements. Furthermore, they thank L. Probst and F. Dimroth for valuable discussions. Also, they would like to thank M. Grave for epitaxial growth, R. Koch for semiconductor processing, T. Dörsam and A. Dilger for packaging support, and M. Schachtner, K. Reichmuth, and G. Siefer for support with electrical measurements.

REFERENCES

- [1] M. Haid, C. Armbruster, D. Derix, C. Schöner, and H. Helmers, “5 W optical power link with generic voltage output and modulated data signal,” in *Proc. 1st Opt. Wireless Fiber Power Transmiss. Conf.*, Yokohama, Japan, 2019, pp. 31–32.
- [2] M. Ishigaki, S. Fafard, D. P. Masson, M. M. Wilkins, C. E. Valdivia, and K. Hinzer, “A new optically-isolated power converter for 12 V gate drive power supplies applied to high voltage and high speed switching devices,” in *Proc. 32nd Ann. IEEE Appl. Power Electron. Conf. Expo.*, Tampa, FL, USA, 2017, pp. 2312–2316.
- [3] X. Zhang *et al.*, “A gate drive with power over fiber-based isolated power supply and comprehensive protection functions for 15-kV SiC MOSFET,” *IEEE J. Emerg. Sel. Topics Power Electron.*, vol. 4, no. 3, pp. 946–955, Sep. 2016.
- [4] F. V. B. de Nazare and M. M. Werneck, “Hybrid optoelectronic sensor for current and temperature monitoring in overhead transmission lines,” *IEEE Sensors J.*, vol. 12, no. 5, pp. 1193–1194, May 2012.
- [5] J. B. Rosolem *et al.*, “Quantitative and qualitative monitoring system for switchgear with full electrical isolation using fiber-optic technology,” *IEEE Trans. Power Delivery*, vol. 30, no. 3, pp. 1449–1457, Jun. 2015.
- [6] P. Antonini *et al.*, “Realization of a high voltage generator by series connection of floating modules,” *Rev. Sci. Instrum.*, vol. 88, no. 2, 2017, Art. no. 25113.
- [7] R. Peña and C. Algora, “One-watt fiber-based power-by-light system for satellite applications,” *Prog. Photovolt: Res. Appl.*, vol. 20, no. 1, pp. 117–123, 2012.
- [8] M. M. Wilkins *et al.*, “Ripple-free boost-mode power supply using photonic power conversion,” *IEEE Trans. Power Electron.*, vol. 34, no. 2, pp. 1054–1064, Feb. 2019.
- [9] M. Röger *et al.*, “Optically powered fiber networks,” *Opt. Express*, vol. 16, no. 26, pp. 21821–21834, 2008.
- [10] H. Miyakawa, Y. Tanaka, and T. Kurokawa, “Design approaches to power-over-optical local-area-network systems,” *Appl. Opt.*, vol. 43, no. 6, pp. 1379–1389, 2004.
- [11] M. Matsuura and J. Sato, “Bidirectional radio-over-fiber systems using double-clad fibers for optically powered remote antenna units,” *IEEE Photon. J.*, vol. 7, no. 1, pp. 1–9, Feb. 2015.
- [12] T. Umezawa, P. T. Dat, K. Kashima, A. Kanno, N. Yamamoto, and T. Kawanishi, “100-GHz radio and power over fiber transmission through multicore fiber using optical-to-radio converter,” *J. Lightw. Technol.*, vol. 36, no. 2, pp. 617–623, Jan. 15, 2018.
- [13] A. Stett, S. Rudorf, R. Rudorf, and H. Helmers, “Implant device having an optical interface,” WO 2018/146032 A1, Aug. 16, 2018.
- [14] K. Goto, T. Nakagawa, O. Nakamura, and S. Kawata, “An implantable power supply with an optically rechargeable lithium battery,” *IEEE Trans. Biomed. Eng.*, vol. 48, no. 7, pp. 830–833, Jul. 2001.
- [15] C. Algora and R. Peña, “Recharging the battery of implantable biomedical devices by light,” *Artif. Organs*, vol. 33, no. 10, pp. 855–860, 2009.
- [16] A. Ahnood *et al.*, “Diamond encapsulated photovoltaics for transdermal power delivery,” *Biosensors Bioelectron.*, vol. 77, pp. 589–597, 2016.
- [17] K. Worms *et al.*, “Reliable and lightning-safe monitoring of wind turbine rotor blades using optically powered sensors,” *Wind Energ.*, vol. 20, no. 2, pp. 345–360, 2017.
- [18] Q. Zhang, W. Fang, Q. Liu, J. Wu, P. Xia, and L. Yang, “Distributed laser charging: A wireless power transfer approach,” *IEEE Internet Things J.*, vol. 5, no. 5, pp. 3853–3864, Oct. 2018.
- [19] H. Helmers, D. Lackner, G. Siefer, E. Oliva, F. Dimroth, and A. W. Bett, “Integrated power and data transceiver devices for power-by-light systems – a concept study,” in *Proc. 32nd Eur. Photovolt. Solar Energy Conf. Exhib.*, Munich, Germany, 2016, pp. 218–222.
- [20] J. Fakidis, S. Videv, H. Helmers, and H. Haas, “0.5-Gb/s OFDM-based laser data and power transfer using a GaAs photovoltaic cell,” *IEEE Photon. Technol. Lett.*, vol. 30, no. 9, pp. 841–844, May 2018.
- [21] D. Derix, R. Freiche, C. Schöner, and A. Hensel, “Comparison of continuous and transition mode in a PV-booster with GaN-transistors and switching frequencies up to 250 kHz,” in *Proc. 17th Eur. Conf. Power Electron. Appl.*, Geneva, Switzerland, 2015, pp. 1–7.
- [22] C. Armbruster, C. Schoener, T. Schoenbett, A. Kloenne, and R. Merz, “Development of a high efficient MPPT for space applications using GaN power transistors,” in *Proc. Int. Exhib. Conf. Power Electron., Intell. Motion, Renewable Energy Energy Manage.*, Nuremberg, Germany, 2017, pp. 451–456.
- [23] Analog Devices, “LTC3425: 5A, 8MHz, 4-Phase synchronous step-up DC/DC converter,” [Online] Available: <https://www.analog.com/en/products/ltc3425.html>. Accessed on: Jan. 24, 2020.
- [24] G. Siefer and A. W. Bett, “Analysis of temperature coefficients for III–V multi-junction concentrator cells,” *Prog. Photovolt., Res. Appl.*, vol. 22, no. 5, pp. 515–524, 2014.
- [25] E. Oliva, F. Dimroth, and A. W. Bett, “GaAs converters for high power densities of laser illumination,” *Prog. Photovolt., Res. Appl.*, vol. 4, no. 16, pp. 289–295, 2008.
- [26] C. L. Schilling *et al.*, “Combining photon recycling and concentrated illumination in a GaAs heterojunction solar cell,” *IEEE J. Photovolt.*, vol. 8, no. 1, pp. 348–354, Jan. 2018.
- [27] H. Helmers *et al.*, “Highly efficient III–V based photovoltaic laser power converter,” in *Proc. 1st Opt. Wireless Fiber Power Transmiss. Conf.*, Yokohama, Japan, 2019, pp. 5–6.
- [28] S. Fafard *et al.*, “High-photovoltage GaAs vertical epitaxial monolithic heterostructures with 20 thin p/n junctions and a conversion efficiency of 60%,” *Appl. Phys. Lett.*, vol. 109, no. 13, 2016, Art. no. 131107.
- [29] S. Fafard *et al.*, “Ultrahigh efficiencies in vertical epitaxial heterostructure architectures,” *Appl. Phys. Lett.*, vol. 108, no. 7, 2016, Art. no. 71101.
- [30] C. Guan *et al.*, “Fabrication and characterization of a high-power assembly with a 20-junction monolithically stacked laser power converter,” *IEEE J. Photovolt.*, vol. 8, no. 5, pp. 1355–1362, Sep. 2018.
- [31] S. K. Reichmuth, H. Helmers, S. P. Philipps, M. Schachtner, G. Siefer, and A. W. Bett, “On the temperature dependence of dual-junction laser power converters,” *Prog. Photovolt: Res. Appl.*, vol. 25, no. 1, pp. 67–75, 2017.
- [32] J. Schubert, E. Oliva, F. Dimroth, W. Guter, R. Löckenhoff, and A. W. Bett, “High-voltage GaAs photovoltaic laser power converters,” *IEEE Trans. Electron Devices*, vol. 56, no. 2, pp. 170–175, Feb. 2009.
- [33] Y. Zhao, Y. Sun, Y. He, S. Yu, and J. Dong, “Design and fabrication of six-volt vertically-stacked GaAs photovoltaic power converter,” *Sci. Rep.*, vol. 6, 2016, Art. no. 38044.
- [34] H. Helmers *et al.*, “Photovoltaic Cells with increased voltage output for optical power supply of sensor electronics,” in *Proc. 17th Int. Conf. Sensors Meas. Technol.*, 2015, pp. 519–524.
- [35] G. Keller *et al.*, “GaAs multi-junction laser power converters at AZUR SPACE: Current status and development activities,” in *Proc. 1st Opt. Wireless Fiber Power Transmiss. Conf.*, Yokohama, Japan, 2019, pp. 11–12.
- [36] R. Kimovec, H. Helmers, A. W. Bett, and M. Topic, “On the Influence of the Photo-Induced Leakage Current in Monolithically Interconnected Modules,” *IEEE J. Photovolt.*, vol. 8, no. 2, pp. 541–546, Mar. 2018.
- [37] R. Kimovec, H. Helmers, A. W. Bett, and M. Topič, “Comprehensive electrical loss analysis of monolithic interconnected multi-segment laser power converters,” *Prog. Photovolt. Res. Appl.*, vol. 27, pp. 199–209, 2019.
- [38] R. Pena and C. Algora, “The influence of monolithic series connection on the efficiency of GaAs photovoltaic converters for monochromatic illumination,” *IEEE Trans. Electron Devices*, vol. 48, no. 2, pp. 196–203, Feb. 2001.
- [39] R. Kimovec, H. Helmers, A. W. Bett, and M. Topič, “Power loss mechanisms in small area monolithic-interconnected photovoltaic modules,” *Opto-Electron. Rev.*, vol. 26, no. 2, pp. 158–164, 2018.
- [40] R. Peña and C. Algora, “Mismatch losses in GaAs monolithically series connected photovoltaic converters for monochromatic illumination,” in *Proc. 16th Eur. Photovolt. Solar Energy Conf.*, Glasgow, U.K., 2000, pp. 1038–1041.
- [41] L. Wagner, A. W. Bett, and H. Helmers, “On the alignment tolerance of photovoltaic laser power converters,” *Optik—Int. J. Light Electron Opt.*, vol. 131, pp. 287–291, 2017.